Applications and Further Developments of Medium Energy Ion Scattering Spectroscopy for Surface and Interface Analysis

D. W. Moon, H. K. Kim, and H. J. Kang*

Surface Analysis Group, Korea Research Institute of Standards and Science, Yousoung P. O. Box 102, Taejon 305-600, Korea

**Department of Physics, Chungbuk National University, Cheongju 360-763, Korea*

(Received September 28 1998; accepted January 11 1999)

Medium Energy Ion Scattering Spectroscopy (MEIS) has been utilized for composition and structure analysis of surface and interface analysis. In this report, it is summarized how MEIS has been used for quantitative depth profiling analysis with atomic depth resolution regarding to preferential sputtering of Ta_2O_5, sputter damage of Si and Pt and Cu single crystals, depth profiling and interface analysis of ultrathin 3-5 nm SiO_2 on Si(001). Application of MEIS for ultrathin film growth with epitaxial Ge on Si(001) with H surfactant and the growth mode change from the layer-by-layer mode to the 3-D mode will be described. Further development of MEIS for atomic scale characterization will be discussed.

1. Introduction

Even though MEIS is not commonly used for surface and interface analysis, it can provide quantitative compositional and structural information with atomic layer depth resolution. Therefore often MEIS analysis results reveal more detailed information on specimen than common surface analysis techniques provide. Sometimes, the information is quite useful for more accurate and meaningful interpretation of results from common surface analysis techniques. Especially, the nondestructive analysis capability of MEIS down to a couple of 10nm subsurface layers with atomic layer depth resolution will be extremely useful to understand and minimize the sputter damage problem commonly encountered in sputter depth profiling. It also makes MEIS a useful tool to analyze surfaces and interfaces of a few nm epitaxial ultrathin films.

In this report, summarized are how MEIS has been used for quantitative depth profiling analysis with atomic depth resolution regarding to preferential sputtering of Ta_2O_5, sputter damage of Si and Pt and Cu single crystals, depth profiling and interface analysis of ultrathin 3-5 nm SiO_2 on Si(001). Application of MEIS for studies of ultrathin film growth of 10 monolayer epitaxial Ge on Si(001) with H surfactant and the layer-by-layer growth and the 3-D growth mode will be described. Further development of MEIS

for atomic scale characterization to analyze light elements and shallow junctions will be discussed.

2. Experimental

Details of the MEIS system at Korea Research Institute of Standards and Science were given elsewhere [2] and a brief description will be given here. In this experiment, 100 keV, 10 nA H^+ ion beams were used and the energy of the scattered H^+ ions were analyzed by a toroidal electrostatic energy analyzer with a two-dimensional position sensitive detector. The base pressure of the MEIS chamber was 5.0×10^{-10} torr but during MEIS analyses, the operating pressure was 5.0×10^{-9} torr.

To measure the damage profile induced by ion beam bombardment in this work, the combined channelling and blocking technique was employed and most of the MEIS spectra for (100) surfaces were taken in the double alignment condition with the channeling and the blocking along the $[11\bar{1}]$ and [111] axial directions corresponding to the incidence angle of 35.3° from the surface normal and the scattering angle of 70.5°. A clean Si(100) surface was obtained by flashing up to 1150°C for 2 min repeatedly. The Si(100) samples were bombarded by 3 keV, 5μ A/cm² Ar^+ ions. The ion incidence angle was varied in the (110) plane. Ta_2O_5 thin films were grwon on Si(001) by MOCVD method. Ge epitaxial layers on Si(001) were grown by e-beam evaporation with dynamic atomic H supply generated by a hot W filament in front of a hydrogen gas doser.

3. Results and Discussions

Shown in Fig. 1 is the altered surface layer of amorphous Ta_2O_5 thin films due to Ar^+ ion bombardment depth profiled nondestructively and quantitatively by MEIS as a function of the ion incidence angle and the ion dose with the depth resolution of better than 1.0 nm. The MEIS spectrum clearly showed preferential sputtering of oxygen atoms. At the steady state under normal incident 3 keV

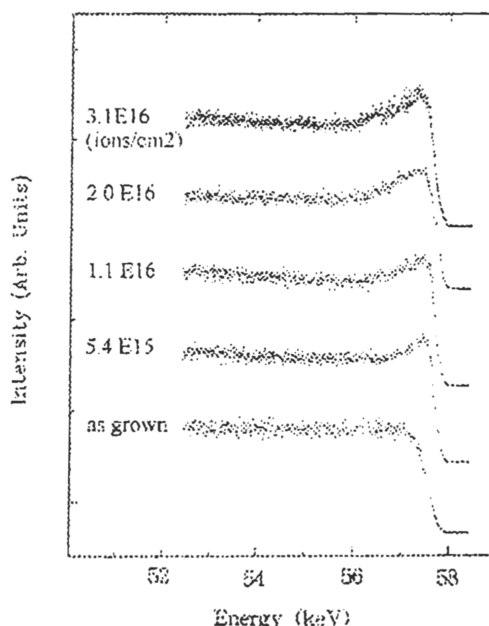

Fig. 1: MEIS spectrum of 30nm Ta_2O_5 shows the preferential sputtering of oxygen due to Ar^+ ion bombardment. The ion energy was 3 keV and the incidence angle was along the surface normal.

Ar^+ ion bombardment, it could be shown with ion scattering analysis program that the composition at the surface changed to $TaO_{0.9}$

and the oxygen depleted thickness was 1.8nm. Preferential sputtering was reduced as the ion incidence angle increased from the surface normal. [2]

To study the damage profile development due to ion bombardment as a function of the ion dose and the ion incidence angle effect on the damage profiles, MEIS spectra were taken from a clean Si(100) surface and ion beam sputtered Si(100) surfaces as shown in Fig.2. [3] MEIS analysis shows that the Si(100) surface layer becomes amorphous initially and the amorphous surface layer gets thicker for a Si(100) surface bombarded with 3 keV Ar^+ ions. The damage profile of the Si(100) saturated at the ion dose of $3x10^{16}$ ions/cm^2 at the incidence angle of 35° from the surface normal. At the saturation ion dose, the depth of the damaged layer was 9.6 nm.

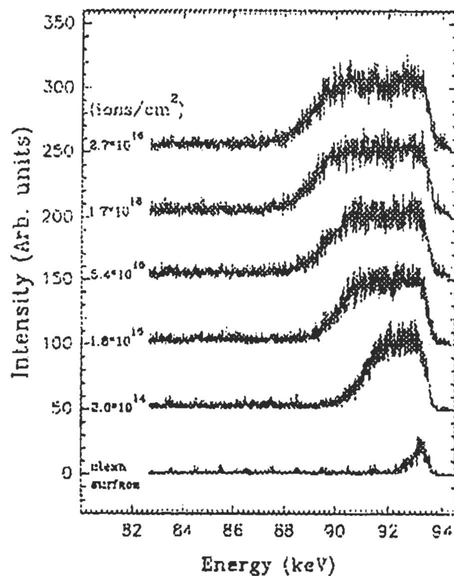

Fig 2: MEIS energy spectrum of Si(100) as a function of 3 keV Ar^+ ion dose. The incidence anlge was 35^0.

The depth of the damaged layer was significantly reduced from 14.2 nm at the surface normal to 4.8 nm at the incidence angle of 80°. Though the depth of the damaged layer was minimized for the sputtering at the extremely glancing angle of 80°, the damaged layer did not disappear but remained as a very shallow surface layer. Similar studies on Pt(111), Cu(111) metallic single crystals showed little radiation damage compared to Si crystals.

To understand the surface oxidation due to the primary oxygen ions commonly used in SIMS analysis, ion beam oxidation of Si(100) was studied with 3 keV O_2^+ ions at room temperature.[4] The change of MEIS energy spectra as a function of 3 keV O_2^+ ion dose are shown in Fig 3. At the ion dose of

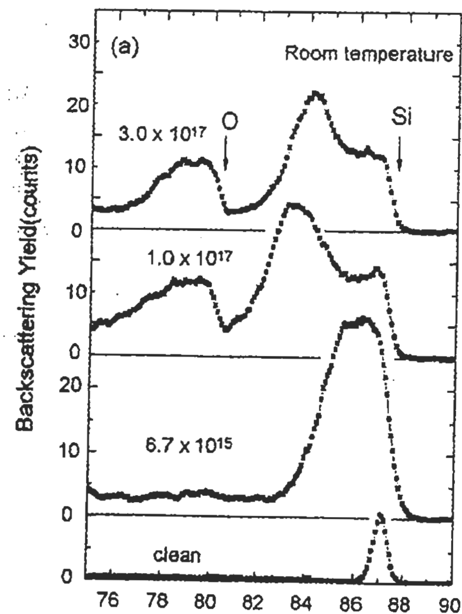

Fig 3: MEIS energy spectrum of Si as a function of 3keV O_2^+ ion dose. The dose unit is oxygen atoms/cm^2.

$5x10^{15}/cm^2$ range, the Si surface becomes amorphous without any formation of an oxidized Si layer. Above $1x10^{17}/cm^2$ ion dose, the MEIS spectrum clearly showed the formation of a SiO_2 layer with a Si suboxide layer and a disordered Si layer in the interface, of which the thickness is 6.7nm, 2.5nm and 3.3 nm, respectively.

The Si(001)-SiO_2 interfaces formed by thermal oxidation and oxygen ion beam oxidation were investigated. [5] The MEIS energy spectra taken in the double alignment condition are given in Fig. 4. Blocking dips around the [111] direction given in Figure 5 were measured with the incident ion beams at 2.5° off from the [00$\bar{1}$]. The energy spectra were fitted by simulations that calculate the energy and intensities of the backscattered particles scattered from thin slabs in the specimen. The program written by Kido *et al.*[6] was modified to treat the crystallinity of each layer with any composition.. The thickness of the interface with (5.5 ± 1.7) $x10^{15}$ Si atoms/cm^2 corresponds to (1.5 ± 0.6) nm considering the volume expansion due to Si oxidation expansion, As can be seen from Fig. 4, there is a transition region with continuously decreasing O density and continuously increasing Si density from the thermal oxide to the Si substrate. The existence of the Si crystalline and its distribution in the transition region can be seen clearly in the presence and the change of the blocking dips in the angular profiles of the Si peak near the [111] direction for three kinds of specimens given in Fig. 5.

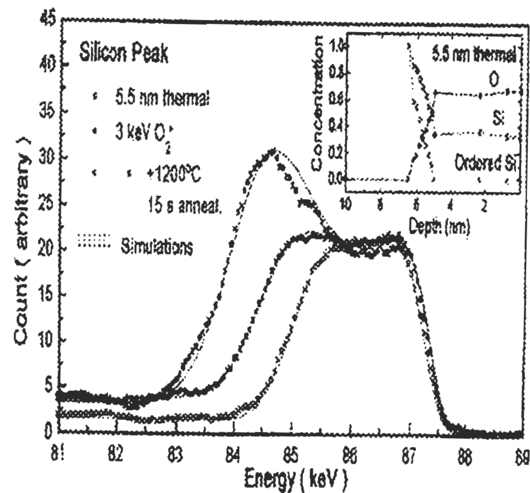

Fig 4. MEIS spectrum of a 5.5nm thermal oxide and an ion beam oxide. The inset is the simulated result.

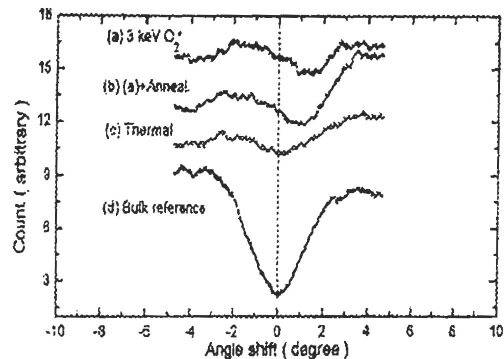

Fig 5. Blocking dips of Si for the thermal oxide, the ion beam oxide, and the bulk Si.

The most interesting and important observation in this experiment is the shifts of the [111] blocking dips to a higher scattering angle in the interface with respect to the dips at the bulk silicon as shown in Fig. 6. However, the [001] blocking dip position at the transition region did not shift from the dip position of the bulk silicon as shown in Fig. 6. From the shift of the blocking dip position, the strain of the crystalline Si lattices could be

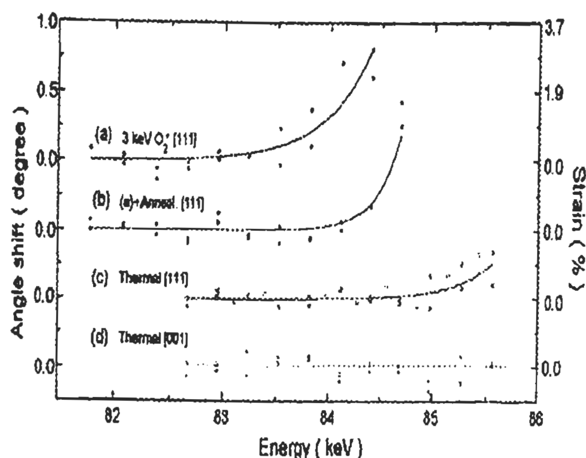

Fig 6: Shift of the [111] blocking dip position and the strain distribution at the SiO_2-Si(001) interface.

estimated and the increase of the strain in the transition region from Si substrate to SiO_2 layer could be measured. The strains were in the vertical direction and the maximum values were 0.96% and 2.8% for thermal oxides and ion beam oxides, respectively.

To study initial stage of epitaxial thin film growth, the scattered ion spectra of Ge overlayers grown on Si(100)-(2 × 1) along a random incidence were taken as shown in Fig 7.[7] The peak at 95.5 keV is the scattered ion yield from surface Ge, and the plateau below 92.8 keV is from the Si substrate. One can notice a big difference between the spectra of the overlayers grown with and without H. In case of the growth without H, the Ge peak remains narrow and the background becomes higher at > 3 ML explaining the growth of 3D hut cluster island. For the growth with H, the Ge peak becomes wider and wider at > 3 ML, suggesting layer-by-layer growth. The same trends were observed up to 10.0 ML. It is possible to conjecture that H etch away the overlayer. In our growing condition, the etching rate was found to be less than 0.05 ML/min (1/20 of the growth rate).

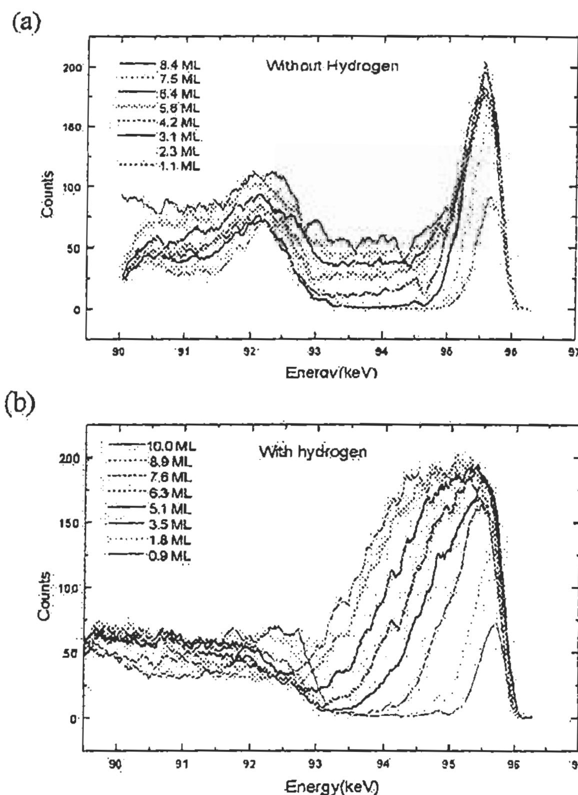

Fig 7: . Energy spectra of scattered ion yield for Ge grown on Si(001) (a) without and (b) with atomic hydrogen. grown at 400 °C with atomic hydrogen fluxes of ~ 2 ML/s.

In order to exploit the strain distribution, we analyzed the blocking dips at various energies at the Ge coverage of 10.0 ML. The blocking dips below 92.8 keV show the strain distributions of the Si substrate below the interface while those above 92.8 keV show that in the Ge overlayer. Their clear shape and minima imply good crystallinity. The angular shift of Ge bloking dip from the

Si one is plotted as a function of the depth for a 10.0 ML Ge overlayer in Fig. 8. For the overlayer grown without H, angular

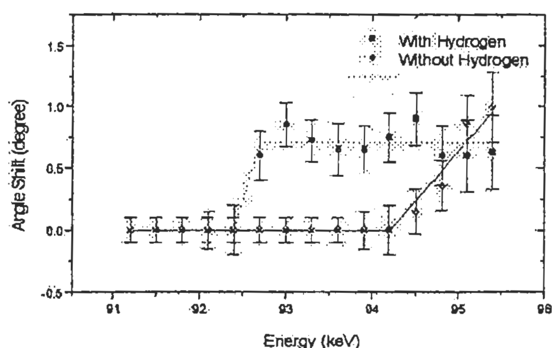

Fig 8: . The angular shift of the Ge blocking dip from the Si one as a function of the depth for a 10.0 ML Ge overlayer grown on Si(001) surface with and without atomic hydrogen.

shift of blocking dip was not observed within the overlayer, suggesting fully relaxed 3D islands with the bulk-like lattice structure were grown. Some shifts near the surface of Ge overlayer can be explained with strained wetting layers in Stranski-Krastanov growth mode. For the overlayer grown with H, the blocking dip for Ge is shifted by ~ 0.7 ° , nearly constant from the interface to the top of the Ge overlayer.

4. Conclusions

In summary, MEIS has been applied to obtain more detailed information on ion-surface interaction such as preferential sputtering and damage profiles. Interface structures below surfaces has been also investigated to get composition profiles and strain distributions. Studies on ion-surface interaction are being extended to ultralow energy ion-surface interactions down to a couple of 1-10eV energy with a low energy ion beam system connected to the MEIS system in line. Understanding ion –surface interaction in the range is very important, because it is presently being used for shallow depth profilng by SIMS and low temperature epitaxial growth. To extend the MEIS analysis capability to low mass elements, direct recoil analysis especially for negative light elements such as H and C are being considered

Acknowledgements:

Financial supports from Center for Molecular Science, Korea and Korea Science and Engineering Foundation(Fund #:976-0200-004-2) are appreciated.

References

1. J.F. van der Veen, Surf. Sci. Rep. 5, 199 (1985).
2. J.C.Lee, C.S.Chung, H.J.Kang, Y.P.Kim, H.J.Kim, D.W.Moon, J.Vac.Sci.Tech., A13,1325-1330 (1995).
3. J.S.Lee, S.C.Jeong, H.J.Kang, H.K.Kim, and D.W.Moon, Applied. Surf. Sci. 100/101. 97-101 (1996).
4. Y.P.Kim, S.K.Choi, Y.H.Ha, S.-H.Kim, H.K.Kim, D.W.Moon, Appl. Surf. Sci., 117/118,207-201 (1997)
5. Y.P. Kim, S. K. Choi, H. K. Kim and D.W. Moon, Appl. Phys. Lett.,71,3504-3506, (1997)
6. Y.Kido and T.Koshikawa, J.Appl.Phys, (67), 187, (1990)
7. S.-J.Kahng, Y.H.Ha,J.-Y.park, S.Kim, D.W.Moon, Y.Kuk, Phys.Rev.Let., 80,4931(1998)